Anatomy, Physiology, and Synaptic Responses of Rat Layer V Auditory Cortical Cells and Effects of Intracellular $GABA_A$ Blockade

BRENDA J. HEFTI AND PHILIP H. SMITH
Department of Anatomy and Neuroscience Training Program, University of Wisconsin Medical School, Madison, Wisconsin 53706

Hefti, Brenda J. and Philip H. Smith. Anatomy, physiology, and synaptic responses of rat layer V auditory cortical cells and effects of intracellular $GABA_A$ blockade. *J. Neurophysiol.* 83: 2626–2638, 2000. The varied extracortical targets of layer V make it an important site for cortical processing and output, which may be regulated by differences in the pyramidal neurons found there. Two populations of projection neurons, regular spiking (RS) and intrinsic bursting (IB), have been identified in layer V of some sensory cortices, and differences in their inhibitory inputs have been indirectly demonstrated. In this report, IB and RS cells were identified in rat auditory cortical slices, and differences in thalamocortical inhibition reaching RS and IB cells were demonstrated directly using intracellular $GABA_A$ blockers. Thalamocortical synaptic input to RS cells was always a combination of excitation and both $GABA_A$ and $GABA_B$ inhibition. Stimulation seldom triggered a suprathreshold response. IB cell synaptic responses were mostly excitatory, and stimulation usually triggered action potentials. This apparent difference was confirmed directly using intracellular chloride channel blockers. Before intracellular diffusion, synaptic responses were stable and similar to control conditions. Subsequently, $GABA_A$ was blocked, revealing a cell's total excitatory input. On $GABA_A$ blockade, RS cells responded to synaptic stimulation with large, suprathreshold excitatory events, indicating that excitation, while always present in these cells, is masked by $GABA_A$. In IB cells that had visible $GABA_A$ input, it often masked an excitatory postsynaptic potential (EPSP) that could lead to additional suprathreshold events. These findings indicate that IB cells receive less $GABA_A$-mediated inhibitory input and are able to spike or burst in response to thalamocortical synaptic stimulation far more readily than RS cells. Such differences may have implications for the influence each cell type exerts on its postsynaptic targets.

INTRODUCTION

Auditory cortex is the last in a series of structures dedicated to the interpretation of auditory input. Many subcortical auditory nuclei have specialized circuits or synapses that have no correlates in the other sensory systems. For instance, the medial nucleus of the trapezoid body (MNTB) contains large calyceal synapses specialized for rapid, precise synaptic transmission (Trussell 1997). Recent evidence (Smith and Populin 1999) suggests that the thalamic input layers of cat auditory cortex may differ from those of visual and somatosensory cortices. It is possible that rat auditory cortex also contains unique circuits and cells specialized for auditory information processing. Alternatively, auditory cortex may process stimuli using circuits similar to those found elsewhere in cortex. It is therefore important to keep these possible specializations in mind and study auditory cortex both in terms of its possible auditory functions and as a part of cerebral cortex.

Sensory cortex influences its targets through a topographically organized descending system originating in layers V and VI, and recent work has begun to elucidate the possible physiological roles of this system (Guillery 1995; Miller 1996; Sherman and Guillery 1996). Layer V is of particular interest because its cells form part of the projection to the thalamus and the entirety of the cortical projection to subthalamic nuclei. In addition, layer V, with cells from all cortical layers (barring layer I), participates in callosal and ipsilateral corticocortical circuits. Layer V has several anatomic and physiological pyramidal cell types and a variety of interneurons (Kawaguchi 1993; Kawaguchi and Kubota 1996). One pyramidal cell type, the intrinsically bursting (IB) cell, is found only in layer V and the deepest region of layer IV in the rat (Connors et al. 1982, 1988; McCormick et al. 1985, somatosensory cortex; Kasper et al. 1994a, visual cortex). The IB cell produces high-frequency bursts of action potentials and is distinguished by its morphology, which is different from that of regular spiking (RS) cells, which also populate layer V (Chagnac-Amitai et al. 1990; Kasper et al. 1994a–c). It is possible that the diverse targets of layer V necessitate a variety of anatomic and physiological response types, but the role of these different types within layer V and their effects on postsynaptic targets are only beginning to be understood (Guillery 1995; Miller 1996; Sherman and Guillery 1996).

In this study we characterized the physiological and anatomic properties of single cells in layer V of primary auditory cortex, their synaptic inputs, and how their responses to these inputs might modulate their cortical and subcortical targets. This report uses three techniques to approach these issues. First, by examining ascending synaptic inputs to layer V cells, latencies, patterns, and degrees of excitation and inhibition can be identified. Second, intracellular blockers of $GABA_A$ allow confirmation of earlier work, which studied the role of inhibition indirectly (Chagnac-Amitai and Connors 1989; Nicoll et al. 1996), as well as further study of the strength of the inhibitory input and its ability to shape the thalamocortical synaptic responses of layer V cells. Third, anatomic results can be correlated to physiological data to give a clearer picture of auditory and more general cortical circuitry. Part of this work

The costs of publication of this article were defrayed in part by the payment of page charges. The article must therefore be hereby marked "*advertisement*" in accordance with 18 U.S.C. Section 1734 solely to indicate this fact.

was published previously in abstract form (Hefti and Smith 1996, 1999).

METHODS

The methods described here for intracellular sharp microelectrode recording are similar to those described previously (Smith 1992). All methods were approved by the University of Wisconsin Animal Care and Use Committee. Animals were maintained in an American Associations for Accreditation of Laboratory Animal Care (AAALAC)–approved facility. Three to 6-wk-old Long-Evans hooded rats were given an anesthetic overdose of chloral hydrate solution (70 mg/ml ip). When areflexive, rats were perfused transcardially with cold, oxygenated sucrose saline (described at end of paragraph). The brain was then exposed dorsally, and cuts in the coronal plane were made halfway through the rostrocaudal extent of the cerebellum and one-third of the way through the rostrocaudal extent of the cerebral cortex. The block of tissue between these two cuts was removed and glued either ventral side down (for horizontal sections) or rostral side down (for coronal sections). The tissue was then submerged in cold, oxygenated saline, and 400- to 500-μm sections were cut through primary auditory cortex (Te1) on a vibratome. To preserve more of the axonal projection from the medial geniculate body (MGB) to Te1 in horizontal slices, the tissue was blocked somewhat higher rostrally and laterally with wedges of fixed egg albumin (Metherate 1999). Sections containing Te1 were placed in a holding chamber containing normal, oxygenated artificial cerebrospinal fluid (ACSF) at room temperature. After equilibrating in the holding chamber for at least 15 min, one slice was transferred to the recording chamber, where it was placed between two pieces of nylon mesh and perfused with normal, oxygenated ACSF at 35°C, which contained the following (in mM): 124 NaCl, 5 KCl, 1.2 KH_2PO_4, 2.4 $CaCl_2$, 1.3 $MgSO_4$, 26 $NaHCO_3$, and 10 glucose. The sucrose saline contained sucrose in place of NaCl (Aghajanian and Rasmussen 1989). The slice was then allowed to rest a minimum of 45 additional minutes before recording began.

Bipolar stimulating electrodes were used to activate axons in the white matter in coronal slices, with stimuli that were stepped from 10 to 150 V in 10-V increments, and with durations of 100 or 200 μs. In horizontal slices, the internal capsule and external capsule were stimulated separately, allowing isolation of thalamocortical from corticocortical inputs (Fig. 1). The space between the paired electrode tips was sufficient to span the width of the fiber tract to stimulate the maximum number of inputs possible. Occasionally, stimulation induced antidromic spikes from the recorded cell. If this was observed, the polarity of the electrode was switched or the stimulating electrode was moved.

Intracellular recordings of responses to injected current and evoked postsynaptic potentials were made with glass microelectrodes of 70–150 MΩ resistance when filled with 2 M potassium acetate and 2% Neurobiotin (Vector Laboratories, Burlingame, CA). Only cells with resting potentials more negative than −60 mV and overshooting action potentials were used for statistical analysis and illustration. Intracellular current and voltage records were digitized with custom software (ICEPAC, L. Haberly, University of Wisconsin). A neuron's membrane potential was calculated by subtracting the cell's recorded voltage from the extracellular DC potential just after exiting the cell. The input resistance was calculated using the slope of the linear portion of the current-voltage plot near the cell's resting potential. Voltage was averaged over 100 ms during the last 120 ms of a 300- or 400-ms current pulse. During recording, Neurobiotin was injected into the cell for ~5 min with 0.4- to 0.6-nA current pulses. To quantify spike half-widths, the first and fifth spikes were measured. The fifth spike was chosen because it was usually the first or second spike after the burst in IB cells, and all cells fired at least five spikes in response to current injection. Measurements were taken at the lowest current injection strength at which the cell fired five spikes, which was always between 0.1 and 0.5 nA. Synaptic latencies were measured from the center of the stimulus artifact, which was usually a total of 0.5 ms in duration, to the onset of the voltage deflection. Inhibitory postsynaptic potential (IPSP) latency was measured from the center of the stimulus artifact to the onset of the IPSP, which was identified as the onset of the change in the slope of the voltage deflection that reversed at levels corresponding to a chloride or mixed anion conductance (usually between −50 and −70 mV).

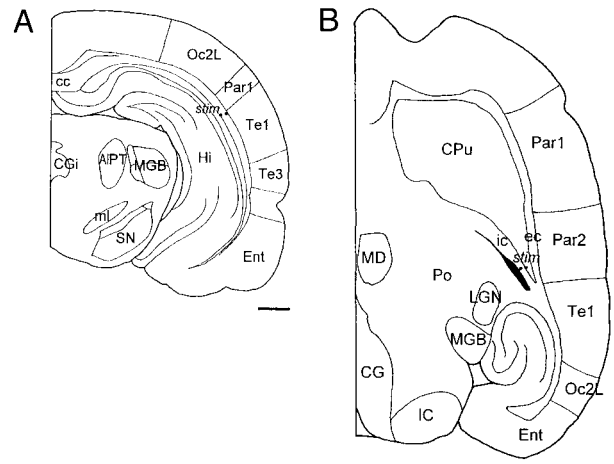

FIG. 1. Drawings of slice preparations. *A*: coronal hemisection illustrating thalamic landmarks and white matter stimulation site (*stim*). All recordings made in area Te1, primary auditory cortex. *B*: semihorizontal section illustrating thalamic and midbrain landmarks and internal capsule stimulation site (*stim*). The tissue is blocked higher rostrally and laterally to give this approximate plane of section. Scale bar is 1 mm. APT, anterior pretectal nucleus; CG, central gray; CPu, caudate putamen; Ent, entorhinal cortex; Hi, hippocampus; IC, inferior colliculus; MD, medial dorsal nucleus; Po, posterior thalamic nucleus; Oc2L, occipital cortex, area 2, lateral; Par1, parietal cortex, area 1; Par2, parietal cortex, area 2; SN, substantia nigra; Te1, primary auditory cortex; Te3, secondary auditory cortex; VP, ventral posterior thalamic nucleus; ec, external capsule; ic, internal capsule; ml, medial lemniscus.

$GABA_B$ was blocked with saclofen (Research Biochemicals International, Natick, MA) in three cells, one IB and two RS. $GABA_A$-activated chloride channels were blocked intracellularly with 5,11,17,23-tetrasulfonato-25,26,27,28-tetramethoxi-calix[4]arene (TS-TM calix[4]arene) and 5,11,17,23-tetrasulfonato-calix[4]arene (TS calix[4]arene), which were generously provided by Dr. Ashvani Singh at the University of Pittsburgh. These compounds were used at a concentration of 1–5 μM. They were injected into the cell after control trials were taken using hyperpolarizing square current pulses (300 ms current pulse every 800 ms). It usually took between 20 and 40 min for the chloride blockers to take effect.

After recording was complete, the slice was fixed in fresh 4% paraformaldehyde. It was then cryoprotected, and 60-μm frozen sections were cut on a freezing microtome and collected in 0.1 M phosphate buffer, pH 7.4. The sections were incubated in avidin-biotin-HRP complex (ABC kit, Vector Labs). The following day, they were rinsed in phosphate buffer and incubated with nickel/cobalt-intensified diaminobenzidine (DAB) (Adams 1981). The sections were then mounted, counterstained with cresyl violet, and coverslipped.

Drawings of injected cells were made using a camera lucida attached to a Zeiss microscope. The location of the cell body relative to the areas of rat cerebral cortex was determined using the atlas of Paxinos and Watson (1986) and studies in which evoked potential recordings were used to map the location of primary auditory cortex (Barth and Di 1990, 1991; Di and Barth 1992). Cells were determined to be within layer V by two means. The first was inspection of individual sections, where differences in cell size, density and shape were used to indicate transitions between cortical layers. The second means to determine laminar borders in Te1 was to use previously established measures of layer V laminar borders (Games and Winer

1988), in which layer V is defined as the region ~51–77% of the distance through Te1 when measured from the pial surface. Only those cells that fell both within primary auditory cortex (Te1) and layer V were used for analysis. Anatomic measurements were made using a Neurolucida drawing system (MicroBrightField, Colchester, VT). All statistical analyses were done using Minitab (Minitab, State College, PA). Depending on the data set, either two-sided two-sample *t*-tests or χ^2 tests were used.

RESULTS

Physiological types in auditory cortex

When cells were recorded from and labeled in layer V of auditory cortex, the large majority showed two distinct patterns of action potential firing (Fig. 2) in response to current pulses. These two patterns have been previously observed in vitro (Agmon and Connors 1989, 1992; Connors et al. 1982, 1988; Kasper et al. 1994a; McCormick et al. 1985) and in vivo in somatosensory (Li and Waters 1996), motor (Baranyi et al. 1993; Pockberger 1991), visual (Holt et al. 1996), and association (Nunez et al. 1993) cortices, and existing terminology has been used here. Most cells showed a RS pattern, which is characterized by a train of single action potentials. In all RS cells, firing begins at a relatively rapid rate, and spike adaptation occurs within the first 50 ms of the current pulse, causing spike frequency to decrease. In 22 of 67 RS cells, denoted RS_1 cells, the cell fires at a constant rate for the remainder of the current pulse (Fig. 2*A*). When hyperpolarized, these cells seldom have a slow depolarization, sometimes called a "sag," and

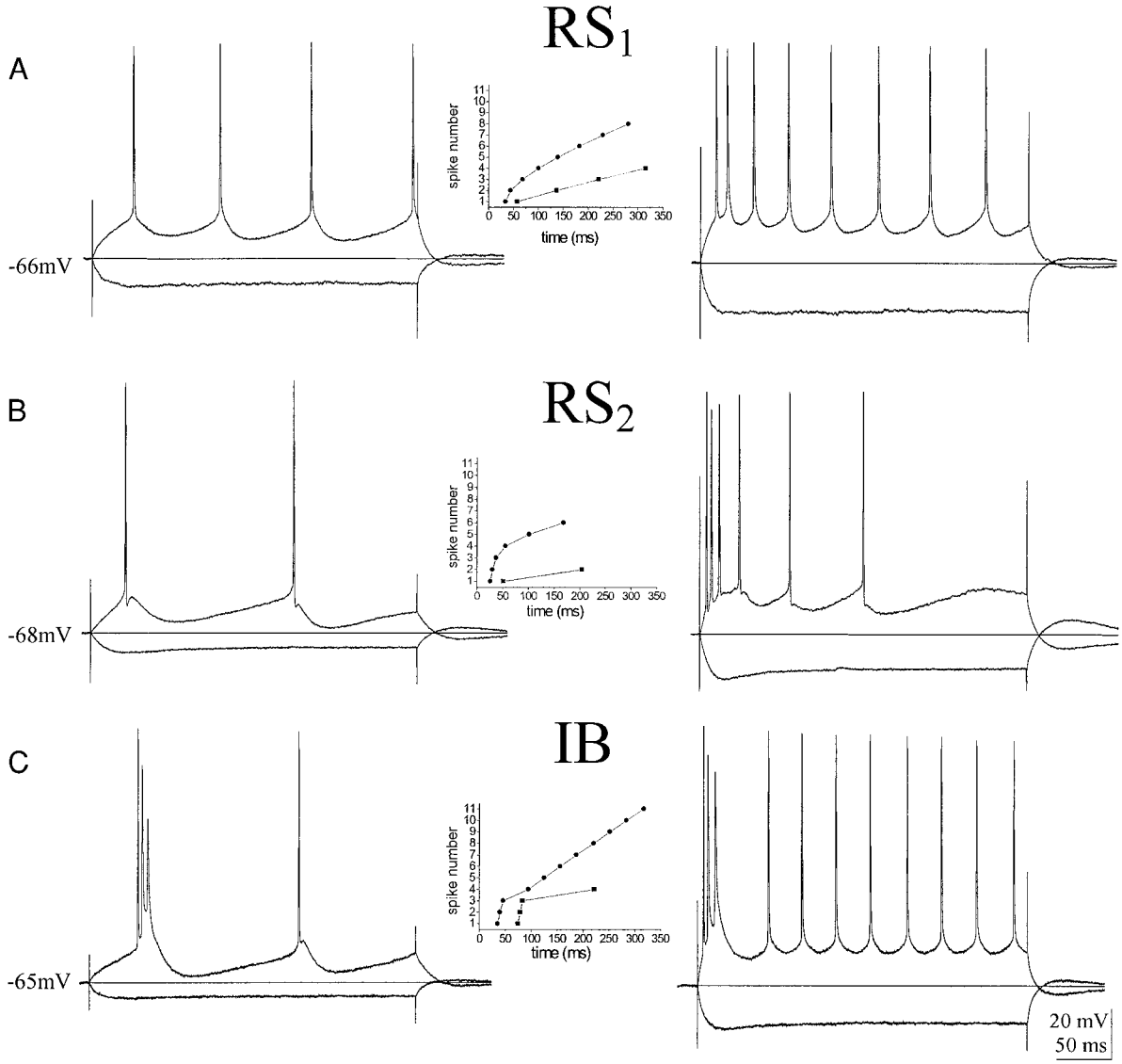

FIG. 2. Intrinsic properties of layer V pyramidal neurons. *A*: intrinsic properties of a regular spiking type 1 (RS_1) cell in response to current injection. Notice early spike frequency adaptation (*right panel*) followed by a sustained firing rate. *Left traces* are responses to ±0.3 nA, and *right* are responses to ±0.6 nA of current. *B*: a regular spiking type 2 (RS_2) cell's intrinsic properties. This cell never maintains a sustained firing rate, and its firing rate slows at higher current injection strengths until it ceases to fire. *Left*: ±0.2 nA. *Right*: ±0.6 nA. *C*: intrinsic properties of an intrinsically bursting (IB) cell. This cell type fires a burst of action potentials that ride on a slower depolarization at the onset of a current pulse and then maintains a steady single spike firing rate. *Left*: ±0.2 nA. *Right*: ±0.6 nA. *Insets*: graphic representations of each cell's firing patterns at low (■) and higher (●) current levels, illustrating changes in interspike interval. Scale bars at *bottom right* apply to all voltage traces.

they have a very small or absent rebound depolarization following the current pulse. A useful way to illustrate firing patterns is to plot spike number against time (Fig. 2*A*, *inset*) (Agmon and Connors 1992). Linear portions of the plot represent a constant firing rate, whereas curved portions illustrate changes in spike rate. RS_1 cells are characterized by a plot that is initially curved and then becomes linear for the majority of the current injection. The remainder (45 of 67) of RS cells were called RS_2 cells. In RS_2 cells, spike rate adaptation continues, and the cell's firing rate slows throughout the current pulse (Fig. 2*B*). In some cases, action potential firing slows until the cell ceases to spike before the current pulse has ended. When hyperpolarized, these cells always showed a slight sag at moderate to large current injection strengths, and they always had a rebound depolarization after the current pulse. The RS_2 cell spike number versus time plot has no linear portion (Fig. 2*B*, *inset*). Although these characteristic differences between RS_1 and RS_2 cells are observable in voltage traces, a satisfactory means to quantify these differences could not be developed. This is most likely because the population of RS_2 cells displayed a range of degrees of spike frequency adaptation, and the classifications RS_1 and RS_2 likely represent opposite ends of a continuum. There were also no significant differences between RS_1 and RS_2 cells in any other intrinsic, synaptic, or anatomic properties that can be analyzed in the slice preparation. These types will therefore be treated as one group, denoted RS, for the remainder of this report.

The other type of pyramidal cell observed in layer V of rat auditory cortex is the IB cell. This cell type fires bursts of three to five action potentials that ride on a slow depolarization at low current injection strengths. At higher current strengths, IB cells fire one such burst at the onset of a current pulse followed by a long hyperpolarization, and then single spikes at a regular rate for the remainder of the current pulse (Fig. 2*C*). When hyperpolarized, these cells often had a sag, but their rebound depolarization was either small or absent. This cell's spike number versus time plot (Fig. 2*C*, *inset*) consists of two separate linear portions of different slopes. Spike frequency within a burst, which averaged 180–200 Hz, was constant across all current injection strengths in an individual cell, and was similar between cells. Spike amplitude decrement was also a consistent feature of the intrinsic burst. The response pattern, burst frequency, and spike decrement observed here are similar to other reports of IB cells (Agmon and Connors 1989; Connors et al. 1982, 1988; Kasper et al. 1994a; McCormick et al. 1985).

The differing intrinsic properties of RS and IB cells are distinguishable on inspection and can be quantified in a number of ways (Table 1). IB cell input resistance was significantly lower than that of RS cells. Spike half-widths were also different between cell types. First and fifth spike half-width were both significantly narrower in IB cells than in RS cells. There was no significant increase in spike half-width in IB cells between their first and fifth spikes, but RS cell spikes did become wider. There was no difference in resting membrane potential between IB and RS cells.

TABLE 1. *Comparisons of IB and RS cell anatomy, intrinsic physiological properties, and synaptic responses*

	RS	IB
V_{rest}, mV	−66.2 ± 4.0	−66.4 ± 4.0
R_{in}, MΩ	49.2 ± 14.7	30.7 ± 8.6*
First spike half-width, ms	0.93 ± 0.25	0.72 ± 0.14*
Fifth spike half-width, ms	1.23 ± 0.46†	0.76 ± 0.15*
EPSP latency, ms	2.8 ± 1.6	2.5 ± 1.6
$GABA_A$ present	50 of 56	16 of 36‡
$GABA_B$ present	50 of 56	1 of 36‡
IPSP latency, ms	4.4 ± 1.7§	3.5 ± 1.1*,§
Fast IPSP ($GABA_A$) reversal, mV	−60.7 ± 3.6	−62.1 ± 5.0
Suprathreshold at rest	16 of 56	27 of 36‡
Soma size, μm^2	145 ± 21	212 ± 22*
Apical dendrite diameter		
50 μm	2.2 ± 0.4	3.8 ± 0.7*
200 μm	2.0 ± 1.3	3.3 ± 0.6*
400 μm	0.8 ± 0.4	2.7 ± 0.4*
Branches from apical dendrite		
Layer V	4.8 ± 2.6	7.9 ± 4.8
Layer IV	3.4 ± 1.8	10.0 ± 3.3*
Layer III	0.8 ± 0.8	5.7 ± 1.9*
Layer II	0.1 ± 0.3	0.8 ± 0.9*
Total branches in layer I	0.6 ± 1.3	13.1 ± 3.4*

Values are means ± SD. Number of RS neurons is 67 and IB neurons is 39. RS, regular spiking; IB, intrinsic bursting; EPSP, excitatory postsynaptic potential; IPSP, inhibitory postsynaptic potential. * Statistically significant difference of at least $P < 0.05$ using a 2 sample *t*-test when comparing the RS cell value to the IB cell value. † Statistically significant ($P < 0.05$) for the comparison of RS cell 1st and 5th spikes. ‡ Statistical significance of at least $P < 0.05$ using a χ^2 test when comparing the RS to the IB cell numbers. § EPSP latencies were significantly shorter ($P < 0.01$) than IPSP latencies in both IB and RS cells.

Anatomic types in auditory cortex

All recorded cells were injected with Neurobiotin and processed for anatomy to study cell morphology. Ten RS cells and 10 IB cells were selected for anatomic analysis. To minimize sampling error and bias, cells from both coronal and horizontal slices were used, they were selected evenly across experimental dates, and no two cells were selected from the same experiment. Qualitatively, the anatomic appearance of RS cells was strikingly different from that of IB cells (Figs. 3 and 4). These differences have been noted previously in other sensory cortices (Chagnac-Amitai et al. 1990; somatosensory and visual cortex; Kasper et al. 1994a–c; visual cortex). The IB cell apical dendrite was very thick and always extended to layer I, where it branched profusely, and it had many dendritic branches in other layers as well. RS cell apical dendrites were shorter and thinner and had fewer secondary branches (Fig. 3). Quantitatively (Table 1), the IB cell soma was much larger than that of RS cells, and the apical dendrite of IB cells was longer. The apical dendrite of IB cells was also consistently thicker than that of RS cells when measured at 50, 200, and 400 μm from the soma. Analysis of the 200- and 400-μm data were complicated by the fact that the RS cell apical dendrite sometimes split into multiple branches, all of which extended toward layer I. Two different measurements were used to compare them with IB cell apical dendrites. In one, only the thickest branch of each RS cell apical dendrite was measured. In the second, all branches of the apical dendrite that continued toward layer I were added together for an individual RS cell and used as a single measure of apical dendritic width. In both cases, the IB cell dendrite was significantly thicker at all distances.

The number of secondary branches in layers II, III, and IV emerging directly from the apical dendrite also differed be-

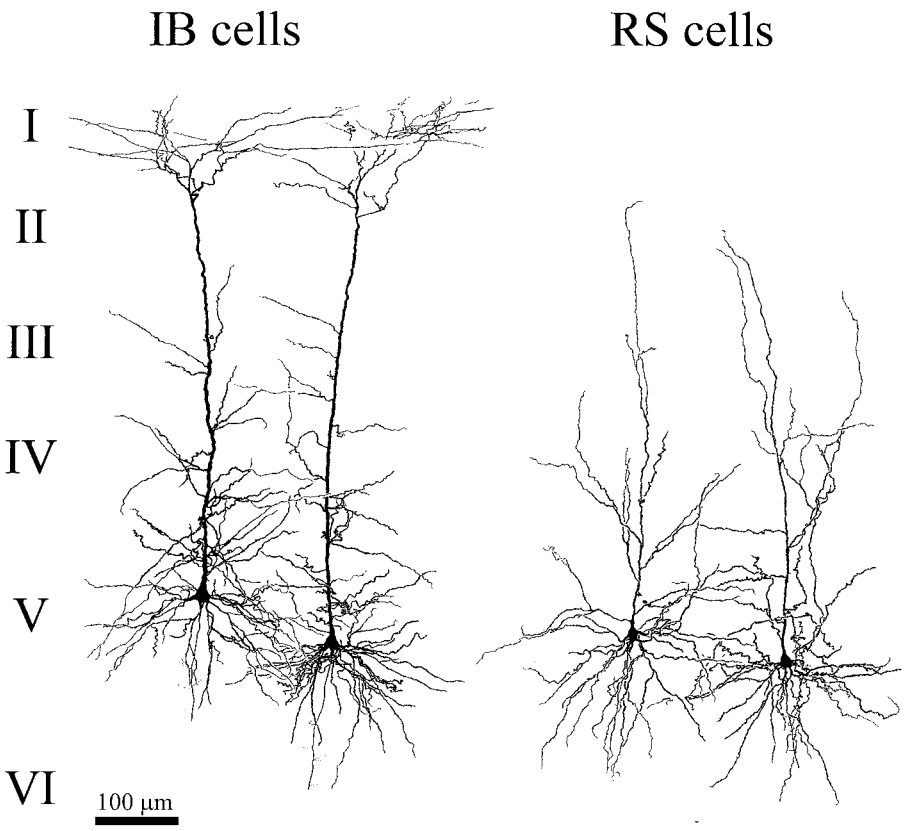

FIG. 3. Camera lucida drawings of IB and RS cell somata and dendrites. Examples of the 2 distinct morphologies displayed by IB and RS physiological types. Notice the significantly larger soma and apical dendrite of the IB cells, as well as the characteristic apical dendritic "tuft," which arborizes extensively in layer I. Axonal arborizations have been eliminated for clarity.

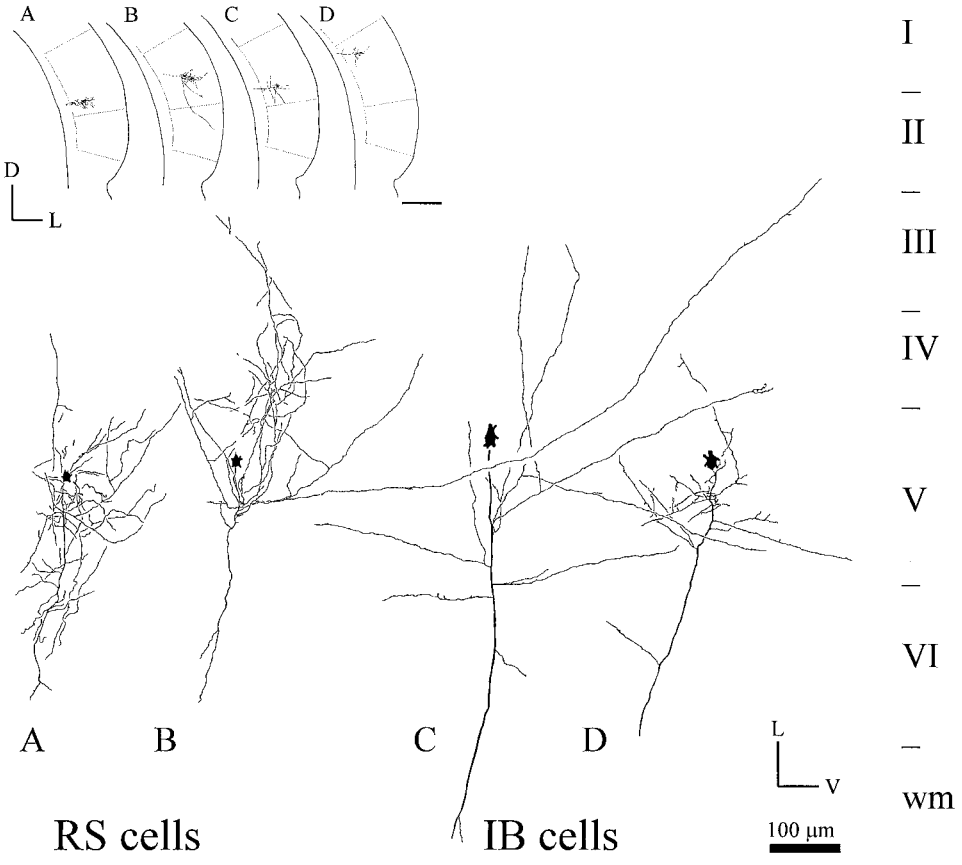

FIG. 4. Camera lucida drawings of IB and RS cell local axonal arborizations. Examples of the 2 distinct patterns of local axonal projections displayed by IB and RS physiological cell types. Soma and primary dendrite initial segments are shown in black, and axons are shown as solid black lines. RS cell (A and B) axons typically arborize in superficial cortical layers (as in B). Occasionally other patterns are seen (A). IB cell (C and D) local axon collaterals can be found in deep cortical layers in all cases. *Inset*: low-magnification drawings illustrating soma location and local axonal arborizations within Te1. Sections are oriented similarly to coronal section shown in Fig. 1, and at the same approximate rostrocaudal level. All cells are located within the borders of Te1, denoted by dotted lines. Ventral to Te1 is Te3, also delineated by dotted lines. Scale bar represents 1 mm.

tween cell types, with IB cells having more branch points in each layer. There was no difference in number of branches in layer V, most likely because of wide variations in soma location within layer V. The distance from the soma to the layer V/IV border in the sampled cells ranged from 10 to 200 μm. All branch points were counted in layer I, and IB cells had significantly more branch points in this layer as well.

These same 20 cells (10 IB and 10 RS) were used for analysis of local axonal arborizations within primary auditory cortex. Results were similar to those seen elsewhere (Mitani et al. 1985; cat auditory cortex; Chagnac-Amitai et al. 1990; Gabbot et al. 1987; Ojima et al. 1992). RS cells had extensive axonal arborizations that were often concentrated in the supragranular layers of cortex (8 of 10 cells; Fig. 4, B). In two cells, axon collaterals were concentrated in layer V and the subgranular layers (Fig. 4, A). Their main axon always extended toward the subcortical white matter, and it was possible in most cases to trace it into the fiber tract (Fig. 4, A and B). The local axons were very thin, and left boutons en passant or at the ends of small stalks. IB cells had fewer local collaterals, and unlike most RS cells, their axonal projections were concentrated in layers V and VI (Fig. 4, C and D). Their main axon could also be followed into the subcortical white matter, and locally projecting axons were thin and left boutons en passant or at the ends of small stalks.

Synaptic responses of RS and IB cells

The plane of section determined which fiber tracts were stimulated in each experiment. In coronal slices, the white matter was stimulated, activating both thalamocortical (TC) and corticocortical (CC) inputs to Te1 (Fig. 1*A*). In horizontal slices, these two pathways were separate, and it was possible to stimulate separately either the TC inputs, in the internal capsule, or the CC inputs, in the external capsule (Fig. 1*B*). Stimulation of the white matter or internal capsule produced similar synaptic responses in RS cells (Table 1). RS cells typically responded first with an excitatory postsynaptic potential (EPSP). The EPSP latency was relatively constant (jitter $<$0.2 ms) in an individual cell, and ranged from 1.5 to 4.0 ms across the RS population. The shortest observed synaptic latencies in this preparation were between 0.5 and 1.0 ms (in IB cells), so it is likely that most RS cell inputs were disynaptic. In a minority of RS cells sampled, this EPSP became suprathreshold at high shock strengths (Fig. 5*Ba*). Most (36 of 56) RS cells could be induced to fire action potentials if they were also depolarized from their resting potential, including all RS cells that also fired an action potential at rest. Some (20 of 56) RS cells never fired an action potential in response to TC or white matter stimulation (Fig. 5*A*). The cells that never spiked received strong inhibition that presumably prevented the membrane voltage from reaching spike threshold.

Following the EPSP in most RS cells was an IPSP, with a latency of 2.0–5.0 ms. The IPSP was visible as a depolarizing PSP and not readily distinguishable from the EPSP at rest, because its reversal potential was more depolarized than the cells' resting potential. Polarizing the cell around its resting potential with current injection during synaptic stimulation revealed a reversal potential that was consistent with a chloride-mediated $GABA_A$ input (Fig. 5*Ac*, $-$60 mV; 5*Bc*, $-$64 mV). A number of attempts were made to confirm that this PSP was mediated by $GABA_A$, but the addition of

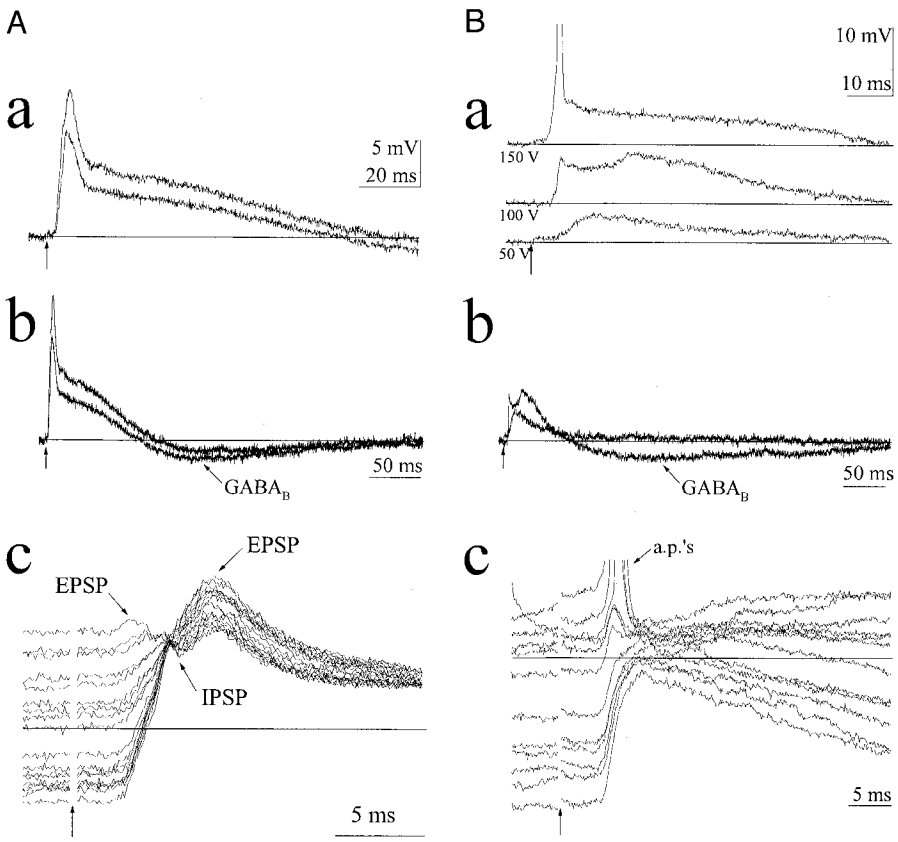

FIG. 5. RS cell synaptic responses to stimulation of the white matter. Examples of synaptic responses to white matter stimulation of 2 different RS cells. Results of white matter stimulation were indistinguishable from internal capsule stimulation. *Aa*: synaptic responses (100 and 150 V) to white matter stimulation at resting potential. $GABA_A$ is depolarizing here, and not easily distinguishable from the excitatory postsynaptic potential (EPSP), as was typical of RS cells. *Ab*: same synaptic responses as illustrated in *Aa*, but shown at a longer time scale to illustrate $GABA_B$. *Ac*: stimulation of white matter input (100 V) while changing the cell membrane potential around rest to illustrate $GABA_A$ reversal, which converges to a single membrane potential. This was typical of RS cells that had strong inhibitory inputs. Horizontal line represents the resting membrane potential of the cell. Voltage scale in *Aa* applies to all 3 traces. *Ba*: another example of an RS cell synaptic response, shown at different intensities to illustrate both supra- and subthreshold responses. Action potential is truncated. *Bb*: subthreshold responses (50 and 100 V) shown at a longer time scale to illustrate emergence of $GABA_B$. *Bc*: polarization of the membrane potential around rest (100 V) to illustrate $GABA_A$ reversal and suprathreshold response when the membrane is depolarized. Action potentials are truncated. Horizontal line represents the resting membrane potential of the cell. Voltage scale in *Ba* applies to all 3 traces. Resting membrane potentials were $-$70 mV (*Aa–Ac*) and $-$63 mV (*Ba–Bc*).

bicuculline to the bath caused global depolarization and uncontrolled spontaneous activity, presumably because of tonic inhibition active in control conditions, making it impossible to record usable data. In many (36 of 56) RS cells, another depolarizing potential could be seen following the IPSP (Fig. 5*Ac*). This second EPSP only occurred when the cell also received inhibition, and it is unclear whether it was a continuation of the initial EPSP, interrupted by the $GABA_A$, or a different input. This second depolarization generally did not trigger an action potential either from resting membrane potential or when the membrane was depolarized. Always associated with the $GABA_A$ in RS cells was a long, slow hyperpolarization, which was likely mediated by $GABA_B$ receptors (Fig. 5, *Ab* and *Bb*). This was confirmed through several experiments in which this hyperpolarization was blocked by saclofen (data not shown). The $GABA_B$ IPSP could be quite large, causing a hyperpolarization of up to 7 mV, and lasting from 300 to 650 ms.

IB cells responded to stimulation of the white matter or internal capsule (in which there are ascending thalamocortical axons, but not corticocortical axons) with an EPSP of 1.5–3.0 ms latency. In a few cases (8 of 36), the synaptic response was suprathreshold except at the very lowest levels of synaptic stimulation (Fig. 6*B*). Many IB cell EPSPs (18 of 36) contained two or three separate components, and unlike in RS cells, the EPSPs did not necessarily occur in the presence of an identifiable IPSP (Fig. 6*A*). In fact, less than half of IB cells received any apparent inhibitory input, which was significantly less often than RS cells. In addition, unlike RS cells, $GABA_A$ was not associated with a $GABA_B$ IPSP. Only one IB cell IPSP appeared to have a $GABA_B$ component, and it was small (<1 mV) and relatively short (225 ms). In a small number of IB cells, internal capsule (TC) stimulation in horizontal slices produced synaptic responses of very short latency (0.5–1.0 ms, $n = 3$ of 10), shorter than any observed during white matter stimulation. This input was always in the form of a single EPSP followed closely by inhibition. The short-latency EPSP and IPSP were both significantly faster than those observed during white matter stimulation ($P = 0.01$). Of the IB cells recorded in this sample, only one seemed to receive both the fast and the slow TC input (not shown). It is certain that portions of the synaptic input to a given cell are missing in any brain slice preparation, so it is possible that a larger number of cells receive both short- and long-latency excitatory input from the thalamus.

No significant differences in PSP latency or amplitude were found between IB and RS cells. Differences between IB and RS cell synaptic responses were found when their more general response properties were compared (Table 1). IB cells were significantly more likely than RS cells to spike or burst in response to synaptic stimulation both at rest and when depolarized. This could be caused by differences in the amount of inhibition each cell type receives overall. IB cells received both $GABA_A$ and $GABA_B$ IPSPs significantly less often than RS cells. The IB cell's greater ability to fire action potentials in response to thalamocortical stimulation and their relative lack of inhibition compared with RS cells were the major findings among the synaptic data.

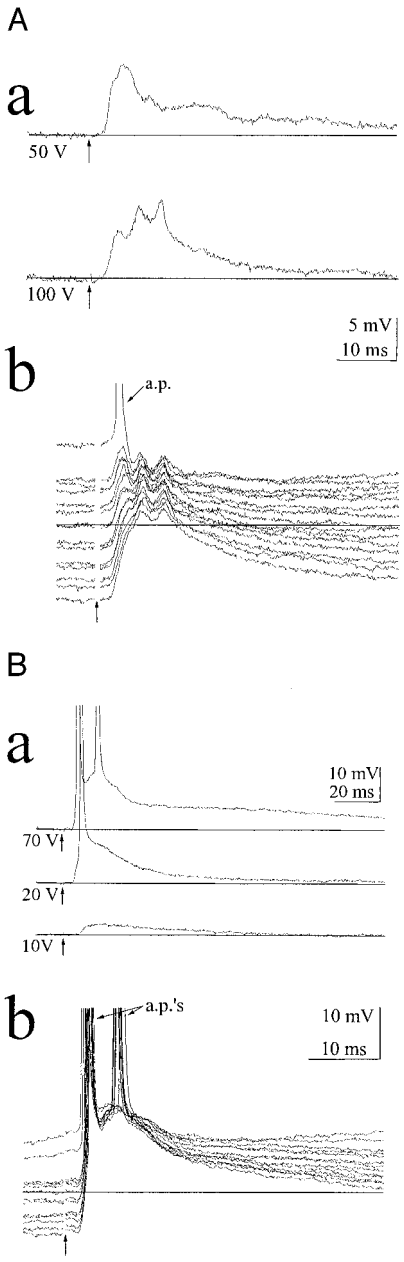

FIG. 6. IB cell synaptic responses to stimulation of the white matter. *Aa*: synaptic response at 2 stimulation strengths to illustrate the 3 components of the response. There was no $GABA_B$. *Ab*: polarization of the membrane around rest to illustrate consistency of this synaptic response and illustrate suprathreshold response with depolarization. The horizontal line represents the resting membrane potential of the cell. Scale bars between *a* and *b* apply to both voltage traces. *Ba*: synaptic response at different stimulation strengths to illustrate transition from subthreshold to single spike to dual spike response. *Bb*: stimulation of the white matter input while polarizing the membrane to different potentials to illustrate inhibition (after 1st spike) and robustness of synaptic response. Horizontal line represents the resting membrane potential of the cell. All action potentials were truncated so that EPSPs are more visible. Resting membrane potentials were −68 mV (*Aa–Ac*) and −64 mV (*Ba–Bc*).

Intracellular $GABA_A$ block with TS-TM calix[4]arene and TS calix[4]arene

We have presented data suggesting that RS cells receive greater inhibition in response to thalamocortical and white matter stimulation than do IB cells. One way to roughly assess the strength of an input is to plot the voltage change it causes

versus the current injected into the cell to hold it at a given voltage. The reversal potential of the input is, by definition, at zero on the *y*-axis. As a cell's membrane potential is moved farther away from this zero point, a rough measure of the strength of this input is how much it is able to change the cell's membrane potential toward its reversal potential. A strong input will cause a change in the membrane potential that is approximately equal to the distance between the cell's membrane potential and the reversal potential of the input. Such inputs often cause "point reversals" such as that seen in Fig. 5*Ac*. Weaker inputs only change the membrane potential a portion of the distance between the cell's membrane potential and the reversal potential of the cell, as in Fig. 5*Bc*. The strength of the input in RS cells versus IB cells has been illustrated in a plot of current injected versus voltage change due to $GABA_A$, in which a steeper slope represents a stronger input (Fig. 7). Only two of each cell type are shown for clarity, but five cells of each type were measured in this way, and the slopes of the RS cell $GABA_A$ inputs were significantly steeper than those of IB cell $GABA_A$ inputs ($P < 0.05$).

To investigate this result further, we sought to pharmacologically isolate excitatory synaptic responses. Use of a bath-applied $GABA_A$ blocker was undesirable for two reasons: first, bath-applied $GABA_A$ blockers at concentrations that totally block that inhibition cause prolonged epileptiform activity in cortical slices. Second, many observed EPSPs, and all of the IPSPs, are probably di- or trisynaptic. Bath-applied blockers would interfere with these circuits before synaptic responses are recorded at the layer V cell, confounding data interpretation. It is possible to block the chloride channels that mediate the $GABA_A$ current intracellularly through addition of TS-TM calix[4]arene and TS calix[4]arene to the recording electrode. These drugs were developed for use in colonic and other tissue for blockade of outwardly rectifying chloride channels (Venglarik et al. 1994), and they have also been shown to block $GABA_A$ receptor channels in visual cortex (Dudek and Friedlander 1996a). Because these compounds take ~30 min to diffuse into a cell, it is possible to record its synaptic responses both before and after the inhibitory chloride channels have been blocked. Another method has also been used to block $GABA_A$ intracellularly (Nelson et al. 1994), but this method, in which cesium is present in the intracellular electrode, has significant effects on the cell's resting membrane potential, input resistance, action potential widths, and level of spontaneous activity. These cellular changes have unknown effects on a cell's responses to synaptic stimuli.

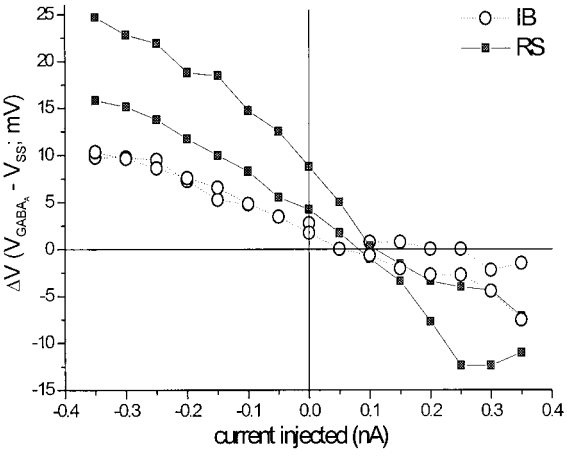

FIG. 7. Comparison of RS and IB cell $GABA_A$ inputs. Plot of current injected vs. the voltage change (voltage change due to $GABA_A$ minus steady-state voltage, in mV) due to $GABA_A$, which is a rough measure of the strength of the synaptic input. RS cells consistently have plots with a steeper slope, indicating a stronger input. Five RS and 5 IB cells were measured in this way, and the slopes of this input were significantly different between groups ($P < 0.05$). Illustrated are 2 cells from each group, RS cells with filled square symbols and generally steeper slopes, IB cells with open circular symbols and shallower slopes.

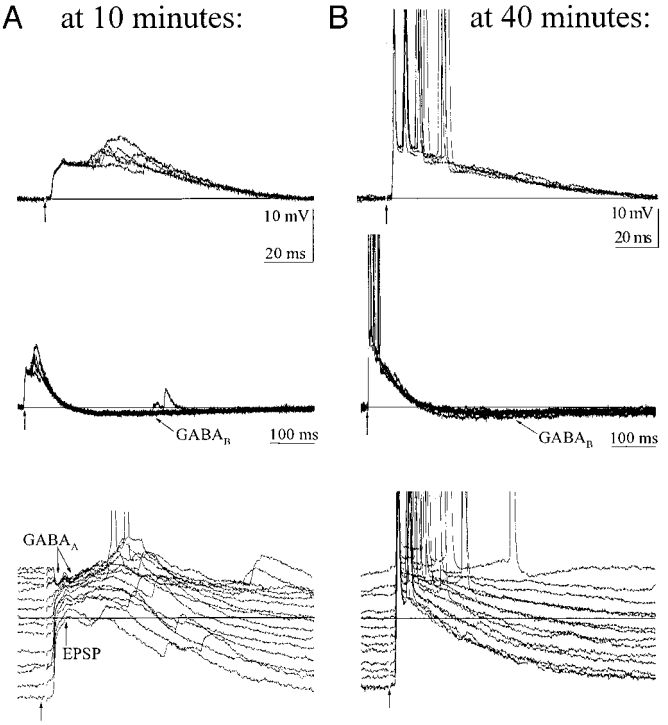

FIG. 8. RS cell white matter synaptic response before and during intracellular $GABA_A$ blockade. *A*: synaptic response of RS cell before chloride channel blockade at a short time scale (*top*), and at a longer time scale (*middle*) to illustrate $GABA_B$ current. *Bottom*: polarization of the membrane around rest during stimulation to illustrate $GABA_A$ synaptic component. Horizontal line represents the resting membrane potential of the cell. *B*: same synaptic response shown after intracellular diffusion of TS-TM calix[4]arene, which blocks $GABA_A$. Synaptic latency is unchanged, but excitatory response has become much larger, producing a series of 3–4 action potentials. The $GABA_B$ component of the inhibition is unchanged. $GABA_A$ appears to be absent on membrane polarization at this stimulus strength (*B, bottom*) and at all other stimulus strengths tested (data not shown). Both voltage and time scales in *A, top* and *B, top* apply to *A, bottom* and *B, bottom*, and voltage scales in *A* and *B, top* apply to *A* and *B, center*. Resting membrane potentials were −75 mV (*A, top, middle*), −70 mV (*A, bottom*), and −68 mV (*B, all*).

As in earlier reports using these drugs (Dudek and Friedlander 1996a,b), no significant changes were observed in any individual cell's resting potential, action potential widths, or input resistance, although cells occasionally displayed spontaneous EPSPs due to an unknown mechanism (data not shown). RS and IB cells had different responses to chloride channel block, but this seemed to be correlated to the apparent strength of the inhibition that was visible at the soma, rather than to cell type. Evoked synaptic responses appeared normal and generated robust $GABA_A$ and $GABA_B$ responses in RS cells (Figs. 8*A* and 9*A*). The $GABA_A$ response was blocked after ~20–60 min of recording, leaving a large excitatory synaptic response ($n = 5$; Figs. 8*B* and 9*C*). The onset of the excitatory response had the same synaptic latency as was observed before $GABA_A$

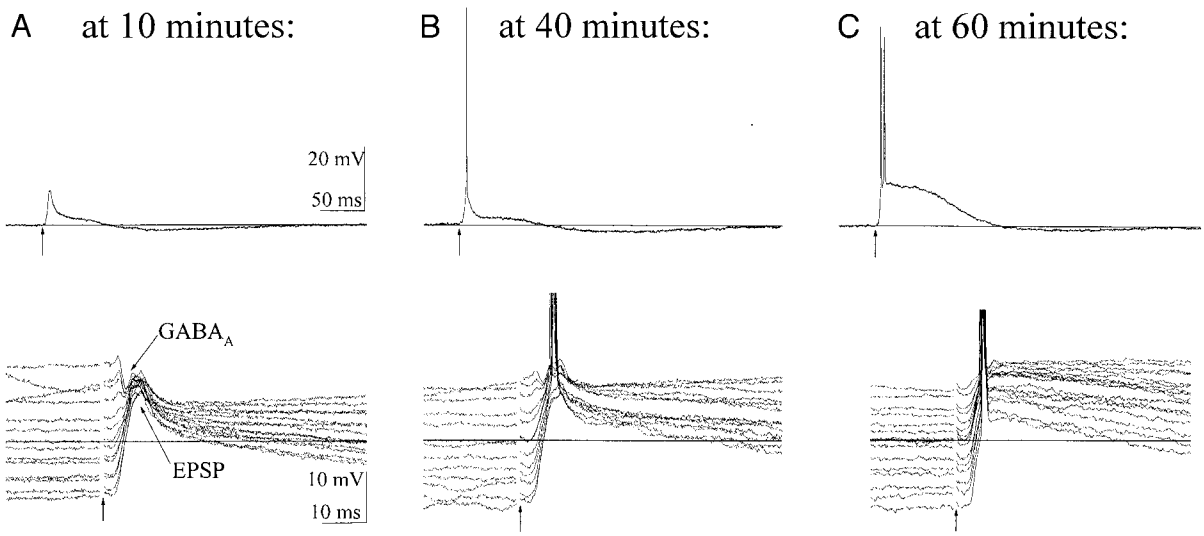

FIG. 9. RS cell white matter synaptic response before and at 2 stages during intracellular $GABA_A$ blockade. Another example of blockade of inhibitory input, showing the transition between normal (*left*) and absent (*right*) inhibitory input. The $GABA_B$ component of the IPSP remains present, but becomes partially obscured at right due to prolonged depolarization in response to synaptic stimulation. Polarization around rest (*bottom traces*) best illustrates gradual blockade of fast inhibition. Horizontal line represents the resting membrane potential of the cell. Action potentials were truncated in the bottom voltage traces in *B* and *C*. Scale bars at *top* and *bottom left* apply to all traces at *top* and *bottom*, respectively. Resting membrane potentials were −70 mV (*A, all*), −66 mV (*B, all*), and −67 mV (*C, all*).

blockade, but the EPSP now caused one or more spikes instead of being shunted by inhibitory input. The $GABA_B$ IPSP remains stable both in amplitude and duration (Figs. 8*B* and 9*C*), indicating that the GABAergic input is still present, but the $GABA_A$ component is blocked. It was also sometimes possible to observe intermediate stages of the $GABA_A$ blockade (Fig. 9*B*). The unveiling of a considerable suprathreshold excitatory event was unexpected, because excitation was not always prominent in the original synaptic responses. On $GABA_A$ blockade, however, the excitatory input was always quite large, consistently causing at least one, and up to four action potentials.

IB cells that lacked an apparent $GABA_A$ input were unaffected by the addition of the chloride channel blocking drugs ($n = 4$; Fig. 10*A*), confirming that recordings of synaptic responses are stable for long periods of time, either in the presence or absence of these compounds. In those IB cells whose evoked synaptic responses contained a $GABA_A$ component ($n = 3$; Fig. 10*B*), it was blocked over a time course similar to that in RS cells. Because IB cells seldom have robust inhibition, the effects of the GABA channel-blocking drugs were less dramatic than was seen in RS cells. These cells often simply produced another action potential where the inhibition had been (Fig. 10*Bb*), without the dramatic changes in synaptic response amplitude and shape often seen in the RS cells.

DISCUSSION

This report represents the first systematic study of the anatomy and physiology of single cells in layer V of auditory cortex. Although part of this work replicates experiments performed elsewhere in cerebral cortex, it is necessary to establish that auditory cortex is organized similarly to other sensory cortices before other properties can be explored. The role of inhibition in shaping the synaptic responses of IB and RS cells has been addressed in a number of ways, and it is the major finding of this report.

Intrinsic and anatomic properties

As reported in other cortical areas, IB cells have large cell bodies and long, thick apical dendrites that branch extensively in layer I. Their axons project into the subcortical white matter and arborize locally in the infragranular cortical layers. RS cells have smaller cell bodies and a thinner apical dendrite that seldom extends to layer I. Their axons also project toward the white matter and arborize locally in supragranular cortex. When injected with current, IB cells fire a characteristic burst of action potentials, followed by either additional bursts or single spikes. RS cells fire single spikes with a variable degree of adaptation. These findings suggest that in layer V, primary sensory cortices share organizational features across sensory modalities.

Thalamocortical input to layer V

Stimulation of the white matter in coronal slices and thalamocortical inputs in horizontal slices produced consistent synaptic responses in both RS and IB cells. When stimulating a fiber tract, there is always the possibility that cortical projection neurons are antidromically activated concurrent with stimulation of thalamocortical fibers. At low and moderate stimulation strengths, it was exceedingly rare to antidromically activate a recorded cell in layer V, or in cells recorded in other cortical layers, although synaptic responses were always observable. This is likely because thalamocortical fibers are thicker than both corticocortical and corticothalamic fibers (Katz 1987; McGuire et al. 1984), and their threshold for activation is lower (Bullier and Henry 1979; Ferster 1990; Ferster and Lindstrom 1983, 1985). Because antidromic spikes were rarely observed, and because low to moderate stimuli

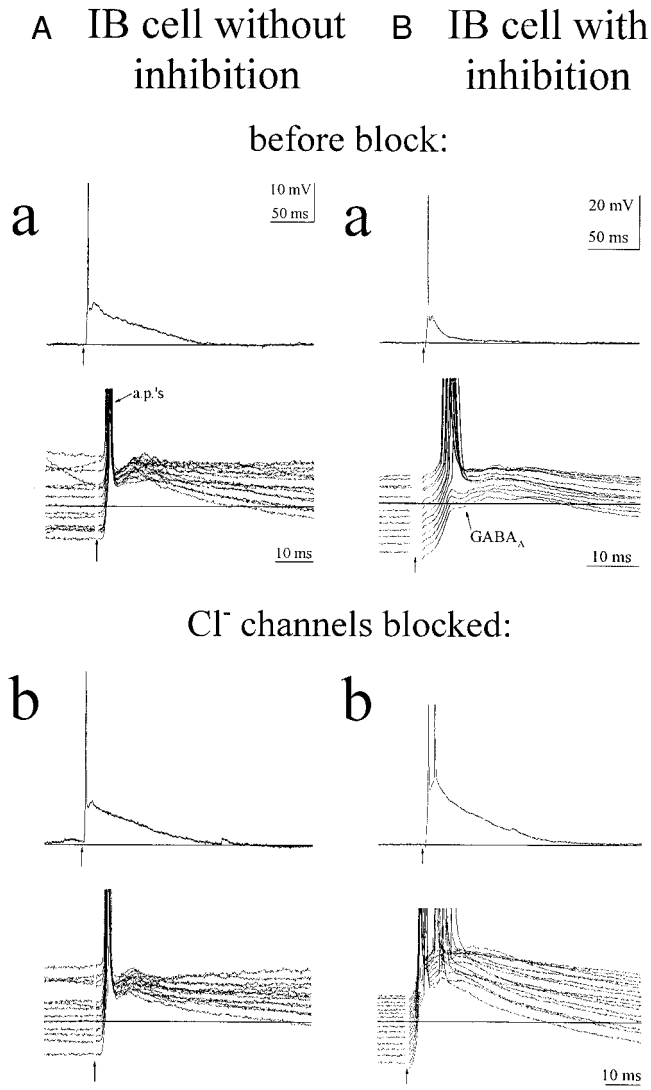

FIG. 10. IB cell white matter synaptic responses in the presence of TS-TM calix[4]arene. *A*: IB cell without apparent inhibition. The synaptic response remains unchanged after >2 h of recording, and after chloride channel blockers are presumed diffused into the cell. Voltage scale at *top* applies to all 4 traces. Time scale at *top* applies to both traces in *Ab*. *B*: IB cell with inhibition. $GABA_A$ is apparent, although partially obscured by the suprathreshold response in the *top 2 panels.* When blocked, another action potential can be seen in response to identical synaptic stimulation in the *bottom 2 panels.* Voltage scale at *top* of *B* applies to all 4 traces. Time scale at *top* also applies to *Bb*, *top*. Resting membrane potentials were −71 mV (*A, all*) and −74 mV (*B, all*).

were generally used, we concluded that the synaptic responses observed are primarily the result of thalamocortical fiber activation.

RS cells received excitation followed by $GABA_A$ and $GABA_B$ IPSPs at latencies indicative of di- or trisynaptic inputs. These RS cell synaptic inputs may have been mediated by cells in layer III/IV receiving direct, suprathreshold thalamic input (Agmon and Connors 1992; Hirsch 1995). Suprathreshold responses were rare unless the cell was depolarized, suggesting that RS cells require concurrent inputs to reach spike threshold. IB cells received excitatory synaptic input either at short latencies, seen only in horizontal slices and suggesting a monosynaptic input, or at longer latencies suggesting a di- or trisynaptic nature. This suggests that thalamocortical input to IB cells can be separated into two channels. The first channel is a fast, probably monosynaptic suprathreshold input. This direct thalamocortical input could arrive on the apical dendrite of the IB cell in layer IV (Kuroda et al. 1995, 1996, 1998). The second channel is a longer latency multicomponent EPSP that may represent input from another IB cell. The EPSP components had the same interevent interval and time course as an IB cell burst, and the multiple-component EPSP was only seen at longer latencies, supporting this speculation. Large layer V cells, morphologically identical to IB cells, are synaptically connected (Gabbott et al. 1987; Markram 1997), also supporting this idea.

Less than half of IB cells received any identifiable inhibitory input, and stimulation usually caused an action potential or burst, even from rest. The difference in the amount of inhibitory input to RS and IB cells was the most striking finding among the synaptic data. IB cells received inhibition less often than RS cells and lacked a $GABA_B$ IPSP. This lack of strong inhibition contributes to the increased ability of IB cells to spike in response to synaptic input in vitro, and may have this effect in the intact system.

Responses of RS and IB cells to stimulation of their synaptic inputs are similar to those observed in other sensory cortices (Baranyi et al. 1993; Chagnac-Amitai and Connors 1989; Nunez et al. 1993). One obvious difference exists between the present findings and a previous study (Agmon and Connors 1992). In that study, most IB cells observed (5 of 7) in somatosensory cortex did not appear to receive any obvious thalamocortical input, which is at variance with the current report. The simplest explanation for this discrepancy is that the stimulation methods used, in which thalamic areas were stimulated, activated a smaller proportion of the total thalamocortical input than the fiber tract stimulation that was used in the current report. In rat motor cortex (Castro-Alemancos and Connors 1996) IB cells appear to receive strong inhibition that can be activated through stimulation of their thalamic inputs. This suggests that pyramidal cells may have different inputs based on the cortical area in which they are found. Differences in inhibition between RS and IB cells have also been observed (Chagnac-Amitai and Connors 1989; Nicoll et al. 1996). Synaptic responses in auditory cortex have been described previously (Cox et al. 1992; Metherate and Ashe 1991, 1993, 1995); however, laminar locations were seldom reported.

IB cells may be well suited to generate synchronized bursts of activity given their relative lack of inhibition (Chagnac-Amitai and Connors 1989). Interconnections exist between IB cells (Markram 1997) and between IB and RS cells (Gil and Amitai 1996), a necessary feature for generating this type of synchronous activity. In addition, some IB cell interburst intervals match the frequency of cortical oscillations observed both in vivo and in vitro, and layer V is both necessary and sufficient to produce synchronous cortical activity (Silva et al. 1991). Our synaptic stimuli revealed inputs to IB cells that matched an IB cell burst in both interevent interval and overall duration, suggesting that at least a portion of the interconnections between IB cells is retained and can be activated in slices.

Intracellular block of $GABA_A$ inhibition

Intracellular $GABA_A$ blockade demonstrated that inhibitory current strength differs between RS and IB cells and confirmed

many earlier experiments in which inhibition was assessed indirectly. Intracellular chloride blockers also revealed a large excitatory event in RS cells, which is not seen under normal conditions. RS cells, on $GABA_A$ blockade, produced a series of action potentials (unlike the IB cell burst, in pattern and frequency), even when the synaptic response formerly contained little discernable excitatory component. The responses of IB cells were less dramatic, often producing an additional spike where an IPSP was formerly seen, or showing no effect in IB cells in which no $GABA_A$ was observed.

These data indicate that the total excitation reaching RS cells is at least as robust as that seen in IB cells. Two questions are whether the inhibitory inputs are activated in vivo to the degree that they are in vitro, and whether they are activated concurrent with the excitation. Intracellular recordings from cat auditory cortex during auditory stimulation in vivo reveal two response types in layers V and VI (Volkov and Galazjuk 1991). Phasic responders, which resemble RS cells in their intrinsic physiology, are excited at tone onset, and thereafter are actively inhibited. Tonic responders, which resemble IB cells physiologically, fired a train of spikes or bursts throughout the tone stimulus. Tonic cells seldom showed inhibition and were more broadly frequency-tuned than phasic neurons. This suggests that the strong, thalamocortically driven inhibition reaching RS cells forms an inhibitory "surround," sharpening RS cell responses. This idea is well established in visual cortex. There, noncorticotectal layer V pyramidal neurons (RS cells) have small receptive fields and narrow orientation and directional selectivity (Finlay et al. 1976; Swadlow 1988). Large layer V corticotectal cells, identified as IB cells (Kasper et al. 1994a; Rumberger et al. 1998), have broader receptive fields and selectivity (Finlay et al. 1976; Swadlow 1988), suggesting that IB cells lack the strong inhibitory input that sharpens RS cell responses to sensory stimuli. The in vivo data fit well with the present findings and indicate that tuning in IB and RS neurons may be shaped by inhibition.

Comparison to in vivo auditory cortical studies

Extracellular studies of auditory cortex reveal neurons sensitive to many aspects of sound stimuli. Some studies note activity described as "bursts" (Evans and Whitfield 1964). Extracellular responses to vocalizations in the squirrel monkey (Glass and Wollberg 1979; Wollberg and Newman 1972) also display spike patterns reminiscent of IB cell bursts, which recur consistently in response to one portion of the call. Although it is impossible to say that the burstlike behavior described above originates from IB cells, it suggests that bursts may be physiologically relevant in the intact system. As previously suggested (Lisman 1997), bursting cells may serve as event detectors. Bursts may also have a higher signal-to-noise ratio and could sharpen frequency tuning (Eggermont and Smith 1996). Clearly more experimentation is needed to characterize the response properties of these bursting cells and to identify them directly with IB cells reported in vitro.

Possible roles of feedback projections from layer V

Anatomic evidence suggests that IB cells are the source of layer V input to the MGB (Winer 1992), inferior colliculus (IC) (Games and Winer 1988; Moriizumi and Hattori 1991), and cochlear nucleus (Weedman and Ryugo 1996a,b). Cells anatomically similar to RS cells project to other cortical areas (Games and Winer 1988), and to the putamen (Ojima et al. 1992).

One unique feature of layer V cells in sensory cortex, identified anatomically as IB cells, is the very large (often >5 μm) synaptic contacts they make in secondary thalamic areas (Bourassa and Deschenes 1995; Hoogland et al. 1991; Roullier and Welker 1991). These contacts may constitute a "driving input" (Guillery 1995; Miller 1996; Sherman and Guillery 1996), in contrast to the layer VI corticothalamic feedback which is "modulatory." In the posterior complex (Po) of somatosensory thalamus, which receives large layer V synaptic contacts, cortical inactivation made cells unresponsive to sensory stimuli (Diamond et al. 1992). This implicates layer V as providing necessary sensory information to secondary thalamic areas and supports the idea that layer V projections are "driving" inputs. The IC receives its cortical input exclusively from layer V. Activating auditory cortex enhances IC cell responses at the peaks of their tuning curves and inhibits responses off-peak (Sun et al. 1996; Yan and Suga 1996). Putative corticocollicular synaptic contacts are small (Saldana et al. 1996), supporting this apparent modulatory role in the IC, although synchronized layer V activity may be capable of driving IC neurons.

The combined anatomic and physiological evidence indicates very different roles for IB and RS cells in cortical and subcortical circuitry. Most RS cells may participate in a feedforward pathway from primary to secondary and contralateral auditory cortices. IB cells, in contrast, make up the majority of layer V's input to subcortical targets such as the MGB and IC and may provide driving inputs in secondary thalamic areas. This creates an alternative corticocortical pathway, through secondary thalamus (Guillery 1995; Sherman and Guillery 1996). Corticothalamocortical synaptic input may be stronger, and therefore more effective, than direct corticocortical projections, as supported by in vivo data and RS cell thalamocortical responses in vitro. Based on evidence from our experiments, RS cells are strongly inhibited and may provide less robust, but perhaps more specific, information about sensory stimuli to their synaptic targets. In contrast, IB cells receive less inhibition and are capable of providing a robust input to any target.

We thank I. Sigglekow, J. Meister, and J. Ekleberry for expert histological processing, Dr. Ashvani Singh for generously providing TS and TS-TM calix[4]arene and helpful comments on its use, and E. Bartlett and M. Banks for discussion of the manuscript and continuing experimental support.

This work was supported by National Institute on Deafness and Other Communication Disorders Grants DC-01999 and DC-00256 and funds provided by a grant to the University of Wisconsin Medical School from the Howard Hughes Medical Institute Research Resources Program for Medical Schools.

Address for reprint requests: P. Smith, Dept. of Anatomy, University of Wisconsin Medical School, 1300 University Ave., Madison, WI 53706.

Received 15 November 1999; accepted in final form 26 January 2000.

REFERENCES

ADAMS, J. C. Heavy metal intensification of DAB-based HRP reaction product. *J. Histochem. Cytochem.* 29: 775, 1981.

AGHAJANIAN, G. K. AND RASMUSSEN, K. Intracellular studies in the facial nucleus illustrating a simple new method for obtaining viable motoneurons in adult rat brain slices. *Synapse* 3: 331–338, 1989.

AGMON, A. AND CONNORS, B. W. Repetitive burst-firing neurons in the deep layers of mouse somatosensory cortex. *Neurosci. Lett.* 99: 137–141, 1989.

AGMON, A. AND CONNORS, B. W. Correlation between intrinsic firing patterns and thalamocortical synaptic responses of neurons in mouse barrel cortex. *J. Neurosci.* 12: 319–329, 1992.

BARANYI, A., SZENTE, M. B., AND WOODY, C. D. Electrophysiological characterization of different types of neurons recorded in vivo in the motor cortex of the cat. II. Membrane parameters, action potentials, current-induced voltage responses and electrotonic structures. *J. Neurophysiol.* 69: 1865–1879, 1993.

BARTH, D. S. AND DI, S. Three-dimensional analysis of auditory-evoked potentials in rat neocortex. *J. Neurophysiol.* 64: 1527–1536, 1990.

BARTH, D. S. AND DI, S. The functional anatomy of middle latency auditory evoked potentials. *Brain Res.* 565: 109–115, 1991.

BOURASSA, J. AND DESCHENES, M. Corticothalamic projections from the primary visual cortex in rats: a single fiber study using biocytin as an anterograde tracer. *Neuroscience* 66: 253–263, 1995.

BULLIER, J. AND HENRY, G. H. Laminar distributions of first order neurons and afferent terminals in cat striate cortex. *J. Neurophysiol.* 42: 1271–1281, 1979.

CASTRO-ALAMANCOS, M. A. AND CONNORS, B. W. Cellular mechanisms of the augmenting response: short-term plasticity in a thalamocortical pathway. *J. Neurosci.* 16: 7742–7756, 1996.

CHAGNAC-AMITAI, Y. AND CONNORS, B. W. Synchronized excitation and inhibition driven by intrinsically bursting neurons in neocortex. *J. Neurophysiol.* 62: 1149–1162, 1989.

CHAGNAC-AMITAI, Y., LUHMANN, H. J., AND PRINCE, D. A. Burst generating and regular spiking layer 5 pyramidal neurons of rat neocortex have different morphological features. *J. Comp. Neurol.* 296: 598–613, 1990.

CONNORS, B. W., GUTNICK, M. J., AND PRINCE, D. A. Electrophysiological properties of neocortical neurons in vitro. *J. Neurophysiol.* 48: 1302–1320, 1982.

CONNORS, B. W., MALENKA, R. C., AND SILVA, L. R. Two inhibitory postsynaptic potentials, and $GABA_A$ and $GABA_B$ receptor–mediated responses in neocortex of rat and cat. *J. Physiol. (Lond.)* 406: 443–468, 1988.

COX, C. L., METHERATE, R., WEINBERGER, N. M., AND ASHE, J. H. Synaptic potentials and effects of amino acid antagonists in the auditory cortex. *Brain Res. Bull.* 28: 401–410, 1992.

DI, S. AND BARTH, D. S. The functional anatomy of middle-latency auditory evoked potentials: thalamocortical connections. *J. Neurophysiol.* 68: 425–431, 1992.

DIAMOND, M. E., ARMSTRONG-JAMES, M., BUDWAY, M. J., AND EBNER, F. F. Somatic sensory responses in the rostral sector of the posterior group (POm) and in the ventral posterior medial nucleus (VPM) of the rat thalamus: dependence on the barrel field cortex. *J. Comp. Neurol.* 319: 66–84, 1992.

DUDEK, S. M. AND FRIEDLANDER, M. J. Intracellular blockade of inhibitory synaptic responses in visual cortical layer IV neurons. *J. Neurophysiol.* 75: 2167–2173, 1996a.

DUDEK, S. M. AND FRIEDLANDER, M. J. Developmental down-regulation of LTD in cortical layer IV and its independence of modulation by inhibition. *Neuron* 16: 1097–1106, 1996b.

EGGERMONT, J. J. AND SMITH, G. M. Burst-firing sharpens frequency-tuning in primary auditory cortex. *Neuroreport* 7: 753–757, 1996.

EVANS, E. F. AND WHITFIELD, I. C. Classification of unit responses in the auditory cortex of the unanesthetized and unrestrained cat. *J. Physiol. (Lond.)* 171: 470–493, 1964.

FERSTER, D. X- and Y-mediated synaptic potentials in neurons of areas 17 and 18 of cat visual cortex. *Visual Neurosci.* 4: 115–133, 1990.

FERSTER, D. AND LINDSTROM, S. An intracellular analysis of geniculo-cortical connectivity in area 17 of the cat. *J. Physiol. (Lond.)* 342: 181–215, 1983.

FERSTER, D. AND LINDSTROM, S. Synaptic excitation of neurons in area 17 of the cat by intracortical axon collaterals of cortico-geniculate cells. *J. Physiol. (Lond.)* 367: 233–252, 1985.

FINLAY, B. L., SCHILLER, P. H., AND VOLMAN, S. F. Quantitative studies of single-cell properties in monkey striate cortex. IV. Corticotectal cells. *J. Neurophysiol.* 39: 1352–1361, 1976.

GABBOTT, P. L., MARTIN, K. A., AND WHITTERIDGE, D. Connections between pyramidal neurons in layer 5 of cat visual cortex (area 17). *J. Comp. Neurol.* 259: 364–381, 1987.

GAMES, K. D. AND WINER, J. A. Layer V in rat auditory cortex: projections to the inferior colliculus and contralateral cortex. *Hear. Res.* 34: 1–25, 1988.

GIL, Z. AND AMITAI, Y. Properties of convergent thalamocortical and intracortical synaptic potentials in single neurons of neocortex. *J. Neurosci.* 16: 6567–6578, 1996.

GLASS, I. AND WOLLBERG, Z. Lability in the responses of cells in the auditory cortex of squirrel monkeys to species-specific vocalizations. *Exp. Brain Res.* 34: 489–498, 1979.

GUILLERY, R. W. Anatomical evidence concerning the role of the thalamus in corticocortical communication: a brief review. *J. Anat.* 187: 583–592, 1995.

HEFTI, B. J. AND SMITH, P. H. Anatomy and physiology of identified rat auditory cortical neurons. *Soc. Neurosci. Abstr.* 22: 1066, 1996.

HEFTI, B. J. AND SMITH, P. H. Anatomy, physiology and synaptic responses of layer V cells in rat auditory cortex: characterization and study of inhibition through intracellular $GABA_A$ blockade. *Soc. Neurosci. Abstr.* 25: 1666, 1999.

HIRSCH, J. A. Synaptic integration in layer IV of the ferret striate cortex. *J. Physiol. (Lond.)* 483: 183–199, 1995.

HOLT, G. R., SOFTKY, W. R., KOCH, C., AND DOUGLAS, R. J. Comparison of discharge variability in vitro and in vivo in cat visual cortex neurons. *J. Neurophysiol.* 75: 1806–1814, 1996.

HOOGLAND, P. V., WOUTERLOOD, F. G., WELKER, E., AND VAN DER LOOS, H. Ultrastructure of giant and small thalamic terminals of cortical origin: a study of the projections from the barrel cortex in mice using Phaseolus vulgaris leuco-agglutinin (PHA-L). *Exp. Brain Res.* 87: 159–172, 1991.

KASPER, E. M., LARKMAN, A. U., LUBKE, J., AND BLAKEMORE, C. Pyramidal neurons in layer 5 of the rat visual cortex. I. Correlation among cell morphology, intrinsic electrophysiological properties, and axon targets. *J. Comp. Neurol.* 339: 459–474, 1994a.

KASPER, E. M., LARKMAN, A. U., LUBKE, J., AND BLAKEMORE, C. Pyramidal neurons in layer 5 of the rat visual cortex. II. Development of electrophysiological properties. *J. Comp. Neurol.* 339: 475–494, 1994b.

KASPER, E. M., LUBKE, J., LARKMAN, A. U., AND BLAKEMORE, C. Pyramidal neurons in layer 5 of the rat visual cortex. III. Differential maturation of axon targeting, dendritic morphology, and electrophysiological properties. *J. Comp. Neurol.* 339: 495–518, 1994c.

KATZ, L. C. Local circuitry of identified projection neurons in cat visual cortex brain slices. *J. Neurosci.* 7: 1223–1249, 1987.

KAWAGUCHI, Y. Groupings of nonpyramidal and pyramidal cells with specific physiological and morphological characteristics in rat frontal cortex. *J. Neurophysiol.* 69: 416–431, 1993.

KAWAGUCHI, Y. AND KUBOTA, Y. Physiological and morphological identification of somatostatin- or vasoactive intestinal polypeptide-containing cells among GABAergic cell subtypes in rat frontal cortex. *J. Neurosci.* 16: 2701–2715, 1996.

KURODA, M., MURAKAMI, K., IGARASHI, H., AND OKADA, A. The convergence of axon terminals from the mediodorsal thalamic nucleus and ventral tegmental area on pyramidal cells in layer V of the rat prelimbic cortex. *Eur. J. Neurosci.* 8: 1340–1349, 1996.

KURODA, M., MURAKAMI, K., KISHI, K., AND PRICE, J. L. Thalamocortical synapses between axons from the mediodorsal thalamic nucleus and pyramidal cells in the prelimbic cortex of the rat. *J. Comp. Neurol.* 356: 143–151, 1995.

KURODA, M., YOKOFUJITA, J., AND MURAKAMI, K. An ultrastructural study of the neural circuit between the prefrontal cortex and the mediodorsal nucleus of the thalamus. *Prog. Neurobiol.* 54: 417–458, 1998.

LI, C. X. AND WATERS, R. S. In vivo intracellular recording and labeling of neurons in the forepaw barrel subfield (FBS) of rat somatosensory cortex: possible physiological andmorphological substrates for reorganization. *Neuroreport* 7: 2261–2272, 1996.

LISMAN, J. E. Bursts as a unit of neural information: making unreliable synapses reliable [see comments]. *Trends Neurosci.* 20: 38–43, 1997.

MARKRAM, H. A network of tufted layer 5 pyramidal neurons. *Cereb. Cortex* 7: 523–533, 1997.

MCCORMICK, D. A., CONNORS, B. W., LIGHTHALL, J. W., AND PRINCE, D. A. Comparative electrophysiology of pyramidal and sparsely spiny stellate neurons of the neocortex. *J. Neurophysiol.* 54: 782–806, 1985.

MCGUIRE, B., HORNUNG, J. P., GILBERT, C. D., AND WIESEL, T. N. Patterns of synaptic input of Layer IV of the cat striate cortex. *J. Neurosci.* 4: 3021–3033, 1984.

METHERATE, R. Intrinsic electrophysiology of neurons in thalamorecipient layers of developing rat auditory cortex. *Dev. Brain Res.* 115: 131–144, 1999.

METHERATE, R. AND ASHE, J. H. Basal forebrain stimulation modifies auditory cortex responsiveness by an action at muscarinic receptors. *Brain Res.* 559: 163–167, 1991.

METHERATE, R. AND ASHE, J. H. Nucleus basalis stimulation facilitates thalamocortical synaptic transmission in the rat auditory cortex. *Synapse* 14: 132–143, 1993.

METHERATE, R. AND ASHE, J. H. Synaptic interactions involving acetylcholine, glutamate, and GABA in rat auditory cortex. *Exp. Brain Res.* 107: 59–72, 1995.

MILLER, R. Cortico-thalamic interplay and the security of operation of neural assemblies and temporal chains in the cerebral cortex. *Biol. Cybern.* 75: 263–275, 1996.

MITANI, A. AND SHIMOKOUCHI, M. Neuronal connections in the primary auditory cortex: an electrophysiological study in the cat. *J. Comp. Neurol.* 235: 417–429, 1985.

MITANI, A., SHIMOKOUCHI, M., ITOH, K., NOMURA, S., KUDO, M., AND MIZUNO, N. Morphology and laminar organization of electrophysiologically identified neurons in the primary auditory cortex in the cat. *J. Comp. Neurol.* 235: 430–447, 1985.

MORIIZUMI, T. AND HATTORI, T. Pyramidal cells in rat temporoauditory cortex project to both striatum and inferior colliculus. *Brain Res. Bull.* 27: 141–144, 1991.

NICOLL, A., KIM, H. G., AND CONNORS, B. W. Laminar origins of inhibitory synaptic inputs to pyramidal neurons of the rat neocortex. *J. Physiol. (Lond.)* 497: 109–117, 1996.

NELSON, S., TOTH, L., SHETH, B., AND SUR, M. Orientation selectivity of cortical neurons during intracellular blockade of inhibition. *Science* 265: 774–777, 1994.

NUNEZ, A., AMZICA, F., AND STERIADE, M. Electrophysiology of cat association cortical cells in vivo: intrinsic properties and synaptic responses. *J. Neurophysiol.* 70: 418–430, 1993.

OJIMA, H., HONDA, C. N., AND JONES, E. G. Characteristics of intracellularly injected infragranular pyramidal neurons in cat primary auditory cortex. *Cereb. Cortex* 2: 197–216, 1992.

PAXINOS, G. AND WATSON, C. *The Rat Brain in Stereotaxic Coordinates.* San Diego, CA: Academic Press, 1986.

POCKBERGER, H. Electrophysiological and morphological properties of rat motor cortex neurons in vivo. *Brain Res.* 539: 181–190, 1991.

ROULLIER, E. M. AND WELKER, E. Morphology of corticothalamic terminals arising from the auditory cortex of the rat: a phaseolus vulgaris-leucoagglutinin (PHA-L) tracing study. *Hear. Res.* 56: 179–190, 1991.

RUMBERGER, A., SCHMIDT, M., LOHMANN, H., AND HOFFMANN, K. P. Correlation of electrophysiology, morphology, and functions in corticotectal and corticopretectal projection neurons in rat visual cortex. *Exp. Brain Res.* 119: 375–390, 1998.

SALDANA, E., FELICIANO, M., AND MUGNAINI, E. Distribution of descending projections from primary auditory neocortex to inferior colliculus mimics the topography of intracollicular projections. *J. Comp. Neurol.* 371: 15–40, 1996.

SHERMAN, S. M. AND GUILLERY, R. W. Functional organization of thalamocortical relays. *J. Neurophysiol.* 76: 1367–1395, 1996.

SILVA, L. R., AMITAI, Y., AND CONNORS, B. W. Intrinsic oscillations of neocortex generated by layer 5 pyramidal neurons. *Science* 251: 432–435, 1991.

SMITH, P. H. Anatomy and physiology of multipolar cells in the rat inferior collicular cortex using the in vitro brain slice technique. *J. Neurosci.* 12: 3700–3715, 1992.

SMITH, P. H. AND POPULIN, L. C. Characterization of cells in cat auditory cortex using an in vitro slice preparation. *Assoc. Res. Otolaryngol. Abstr.* 22: 117–118, 1999.

SUN, X., CHEN, Q. C., AND JEN, P. H. Corticofugal control of central auditory sensitivity in the big brown bat, *Eptesicus fuscus. Neurosci. Lett.* 212: 131–134, 1996.

SWADLOW, H. A. Efferent neurons and suspected interneurons in binocular visual cortex of the awake rabbit: receptive fields and binocular properties. *J. Neurophysiol.* 59: 1162–1187, 1988.

TRUSSELL, L. O. Cellular mechanisms for preservation of timing in central auditory pathways. *Curr. Opin. Neurobiol.* 7: 487–492, 1997.

VENGLARIK, C. J., SINGH, A. K., AND BRIDGES, R. J. Comparison of -nitro versus -amino 4,4′-substituents of disulfonic stilbenes as chloride channel blockers. *Mol. Cell. Biochem.* 140: 137–146, 1994.

VOLKOV, I. O. AND GALAZJUK, A. V. Formation of spike response to sound tones in cat auditory cortex neurons: interaction of excitatory and inhibitory effects. *Neuroscience* 43: 307–321, 1991.

WEEDMAN, D. L. AND RYUGO, D. K. Pyramidal cells in primary auditory cortex project to cochlear nucleus in rat. *Brain Res.* 706: 97–102, 1996a.

WEEDMAN, D. L. AND RYUGO, D. K. Projections from auditory cortex to the cochlear nucleus in rats: synapses on granule cell dendrites. *J. Comp. Neurol.* 371: 311–324, 1996b.

WINER, J. A. The functional architecture of the medial geniculate body and the primary auditory cortex. In: *The Mammalian Auditory Pathway: Neuroanatomy.* New York: Springer-Verlag, 1992, p. 222–409.

WOLLBERG, Z. AND NEWMAN, J. D. Auditory cortex of squirrel monkey: response patterns of single cells to species-specific vocalizations. *Science* 175: 212–214, 1972.

YAN, J. AND SUGA, N. The midbrain creates and the thalamus sharpens echo-delay tuning for the cortical representation of target-distance information in the mustached bat. *Hear. Res.* 93: 102–110, 1996.